

## ULTRA-WIDEBAND CAVITY-BACKED BOWTIE ANTENNA FOR PATTERN IMPROVEMENT

Zhiya Zhang<sup>1, \*</sup>, Shaoli Zuo<sup>2</sup>, Xiaolu Zhang<sup>1</sup>, and Guang Fu<sup>1</sup>

<sup>1</sup>National Laboratory of Science and Technology on Antennas and Microwaves, Xidian University, Xi'an, Shaanxi 710071, China

<sup>2</sup>School of Science, Xidian University, Xi'an, Shaanxi 710071, China

**Abstract**—The design and ultra-wideband performance of a cavity-backed bowtie antenna with the parasitic dipole and parasitic circular ring is presented. Besides the elliptical bowtie dipole and the taper feeding microstrip for obtaining ultra-wideband impedance characteristics, the parasitic dipole and parasitic circular ring to effectively improve the radiation pattern can be used for obtaining the stable broadside unidirectional radiation patterns. An ultra-wideband impedance characteristic of about 118.2% for  $VSWR \leq 2$  ranging from 2.75–10.7 GHz is achieved. A unidirectional radiation pattern, a stable peak gain of around 7.4–10.8 dBi and low cross polarization over the whole operating band are also produced. A prototype has been fabricated and tested, and the experimental results validate the design procedure.

### 1. INTRODUCTION

The need of ultra-wideband (UWB) applications in the near future draws the attention of the scientific community because of its unlimited applications in short-range wireless communication, localization and tracking, medical imaging and monitoring and many more [1–4]. According to UWB definition of FCC, the UWB has wide spectrum (3.1 GHz–10.6 GHz) [5]. Many UWB antennas have been discussed in the literatures to fulfill this requirement [6–14], where short range and extremely wide bandwidth antennas were needed. Indoor wireless networks consisting of numerous indoor antennas have been mounted on the ceiling of many buildings and malls,

---

*Received 9 November 2012, Accepted 5 January 2013, Scheduled 10 January 2013*

\* Corresponding author: Zhiya Zhang (zhiyazhang@163.com).

which stringent requirements on antenna's wide impedance bandwidth, low profile and unidirectional radiation patterns are needed [15, 16]. Actually, low-profile antenna capable of UWB operation, with stable unidirectional radiation patterns is difficult to design. Monopole and microstrip antennas are attractive for present wireless communication systems because they can provide wideband impedance characteristics easily [17, 18], however, the radiation patterns at higher frequency band are to be distorted. Cavity-backed antenna for unidirectional radiation have recently been demonstrated [19–23]. This design has the advantage of obtaining unidirectional radiation pattern with high gain, low sidelobe and backlobe. By locating a cavity backed on an open sleeve dipole antenna, stable unidirectional radiation patterns and 10 dBi gain are obtained but with a 55% impedance bandwidth only [21]. In [22, 23], a cavity-backed folded triangular bowtie antenna and a cavity-backed triangular bowtie dipole antenna have also achieved unidirectional radiation patterns and with an impedance bandwidth of 92.2% and 91.4% for  $VSWR \leq 2$ , respectively. However, the available bandwidth of antennas with cavity-backed structures is often limited by their distorted radiation patterns at higher frequency band.

In this paper, we propose a design of a cavity-backed bowtie antenna with the parasitic dipole and parasitic circular ring. Using the parasitic dipole and parasitic circular ring to effectively improve the radiation patterns, the proposed antenna can achieve a stable broadside unidirectional radiation patterns in the whole operation bands. In particular, ultra-wideband impedance characteristic of about 118.2% for  $VSWR \leq 2$  ranging from 2.75–10.7 GHz is also obtained by the elliptical bowtie dipole and the taper feeding microstrip. With this good ultra-wideband and stable unidirectional radiation pattern performance, it is an excellent candidate for the indoor applications of the recent wireless communication services.

## 2. ANTENNA DESIGN

A 3D perspective of the proposed antenna and coordinate system are shown in Figure 1(a). The antenna mainly comprises an elliptical bowtie dipole, a parasitic elliptical bowtie dipole, a taper microstrip feeding, two parasitic circular rings a composite cavity and the plastic posts. Figures 1(b) and (c) show the side view and detail view of the proposed antenna. From the figures, it can be seen that there are three layers which including the upper substrate layer, the lower substrate layer and the ground plane with the diameter of  $D_g$ . The both substrates with permittivity of 2.65, loss tangent of 0.003, a radius

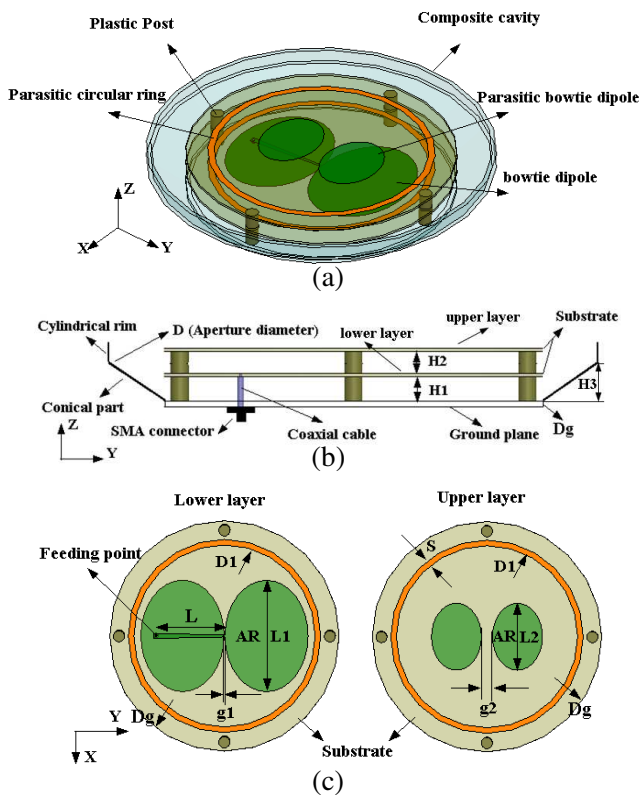


**Figure 1.** Geometry of proposed design: (a) 3D view. (b) Side view. (c) Detail view.

of 62 mm, and a thickness of 1 mm are supported by the plastic posts. By etching the elliptical bowtie dipole with the major diameter of  $L_1$  and the ratio of 0.75 ( $AR$ ) on the opposite plane of the lower substrate layer, the wideband impedance characteristic is achieved. The parasitic elliptical bowtie dipole with the major diameter of  $L_2$ , the ratio of 0.75 ( $AR$ ) is printed in the upper plane of the upper substrate layer, which can be used for improving the radiation patterns for higher bands. Moreover, the two parasitic circular rings with the diameter of  $D_1$ , the width of  $S$  printed in the upper planes of the two substrates, respectively, are also successfully employed to improve the radiation pattern for higher bands. The gaps between the two arms of the elliptical bowtie dipole and the parasitic elliptical bowtie dipole are the dimension of  $g_1$  and  $g_2$ , respectively, which can be used for tuning the impedance matching.



**Figure 2.** Photograph of the proposed antenna.

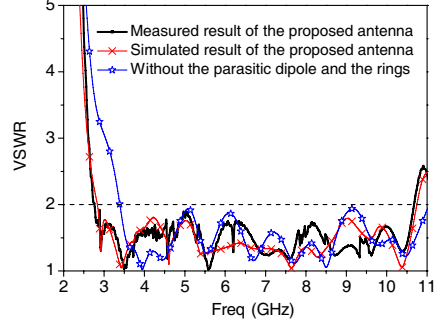


**Figure 3.** Simulated and measured VSWR against frequency.

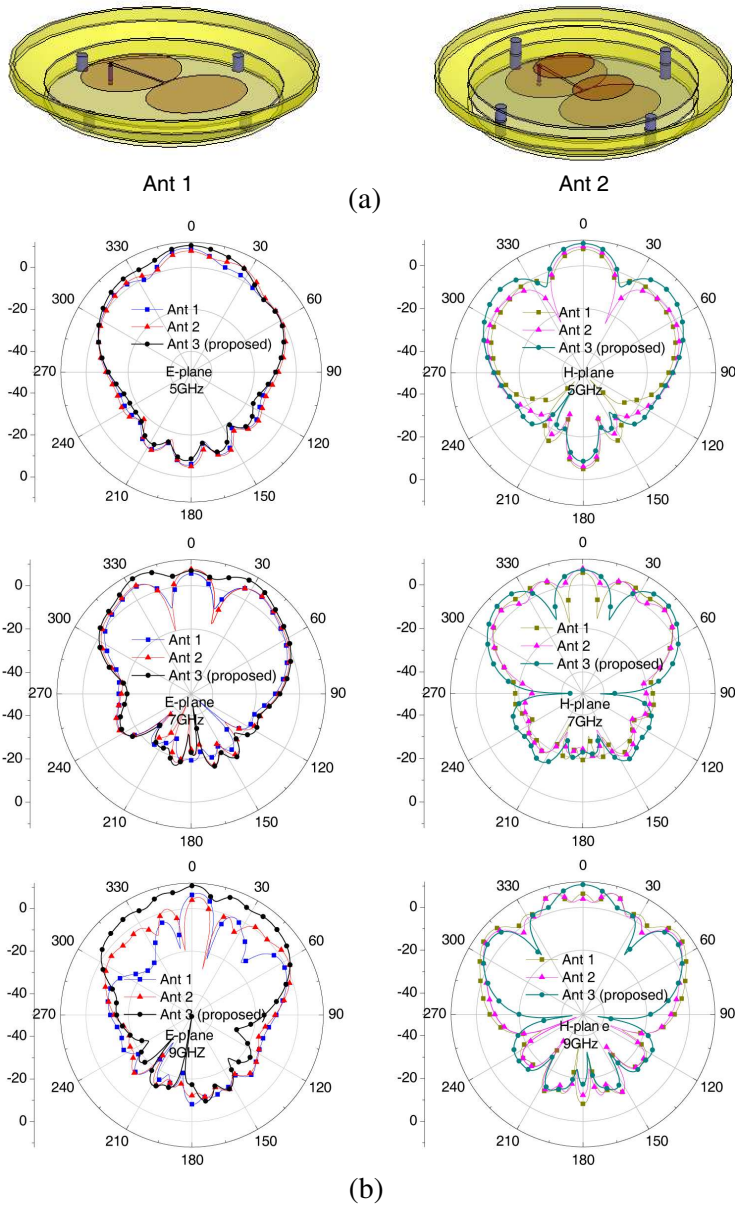
**Table 1.** Dimensions of the proposed antenna.

Parameters	$D$	$D_g$	$D_1$	$L$	$L_1$	$L_2$	$g_1$	$g_2$	$H_1$	$H_2$	$H_3$	$S$	$AR$
Values/mm	160	120	98	39.2	64	36	0.4	6	8	7	12	3	0.75

The feed mechanism is designed into two parts: the taper microstrip line and the coaxial cable. The taper microstrip line printed in the upper plane of the lower substrate layer with the length of  $L$  which the impedance varying from  $50\Omega$  to  $88\Omega$  for impedance matching is feed to an arm of the elliptical bowtie dipole directly. The coaxial cable connected to the SMA can be used to feed the antenna which the inner conductor connects to the taper microstrip line and the outer conductor connects to the other arm of the elliptical bowtie dipole. The cavity consists of a conical part with the height of  $H_3$  and a cylindrical rim with the diameter of  $D$  which determines the antenna aperture. By introducing the cavity, the unidirectional radiation pattern of the antenna is obtained. The final optimal antenna parameters are shown in Table 1. A prototype of the proposed antenna was fabricated according to these design parameters, as shown in Figure 2.

### 3. RESULTS AND DISCUSSION

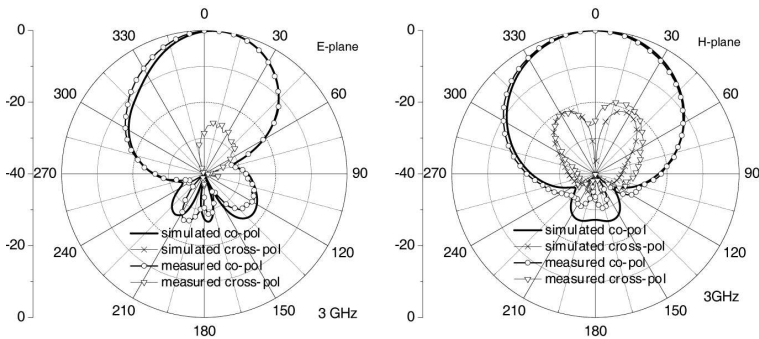
The impedance characteristics of the antenna were simulated using the Ansoft High-Frequency Structure Simulator (HFSS.13) simulation software, and the measured results obtained with Agilent E8363B network analyzer and an anechoic chamber. Figure 3 shows the measured and simulated VSWR for the antenna. For  $VSWR \leq 2$ , the



**Figure 4.** Comparison between simulated RP without the parasitic dipole and the parasitic circular rings (Ant 1), without the parasitic circular rings (Ant 2) and the proposed antenna (Ant 3): (a) Antenna structures; (b) Simulated results.

measured impedance bandwidths are about 118.2% (2.75–10.7 GHz) which covering the UWB operation bands and has good agreement with the simulation. Compared with the VSWR without the parasitic dipole and the parasitic circular rings, it is noted that the impedance bandwidth characteristic is not affected mostly; however, a small improvement for lower band is obtained.

Figure 4 shows the simulated radiation patterns (RP) in the  $E$ - and  $H$ -planes at 5, 7 and 9 GHz for the proposed antenna, denoted as Ant 3. With the cavity backed on the antenna, obviously, it can be seen that the unidirectional radiation patterns are obtained in the operation bands. Meanwhile, to examine the effects of the parasitic elliptical bowtie dipole and the two parasitic circular rings to the antenna's radiation patterns, the simulated results of RP for the case without the parasitic elliptical bowtie dipole and the two parasitic circular rings (denoted as Ant 1) and the case without the two parasitic circular rings (Ant 2) were also studied and plotted in Figure 4(b). The geometries of the two studied antennas are shown in Figure 4(a), and their corresponding dimensions are the same. Obviously, for the case without the parasitic elliptical bowtie dipole and the two parasitic circular rings, the distortion of the radiation patterns and the lower gain in the upper band (at 7 and 9 GHz) is clearly observed from the figure, which due to the length of the dipole arm is more than  $0.7\lambda$  at high frequencies and the currents of the higher order modes along the two radiating arms are out of phase that give rise to the change of the radiation patterns and the cancellation of radiation that eventually limits the achievable maximum gain. Furthermore, in order to advance the radiation patterns, by disposing the parasitic elliptical bowtie dipole at the upper plane of the upper substrate layer, the Ant 2 is formed. In this case, improvement for radiation patterns and great increase in boresight gains especially at higher frequencies are obtained. When the two parasitic circular rings are further added to



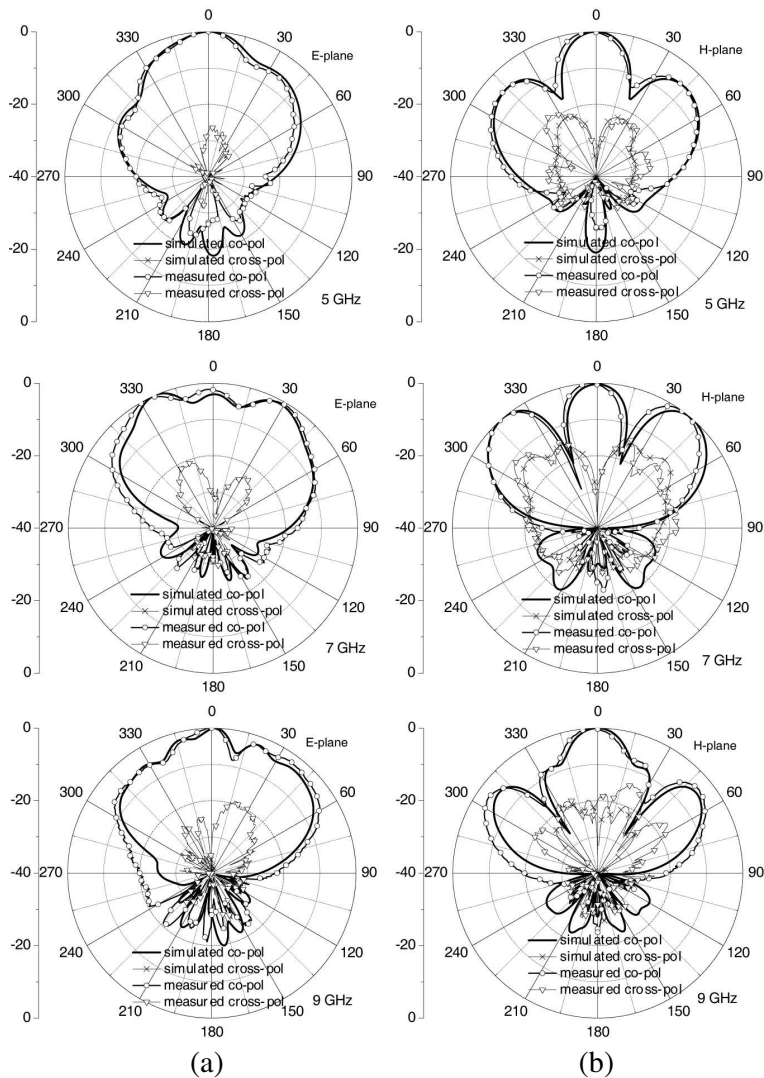


**Figure 5.** Simulated and measured radiation patterns at 3, 5, 7 and 9 GHz: (a) *E*-plane. (b) *H*-plane.

Ant 2, the Ant 3 for the proposed antenna is formed. It can be seen that the radiation patterns become fatter, smoothness and the peak gain is improved in high frequency band.

The measured and simulated radiation patterns of the co-polarization and the cross-polarization for the proposed antenna in

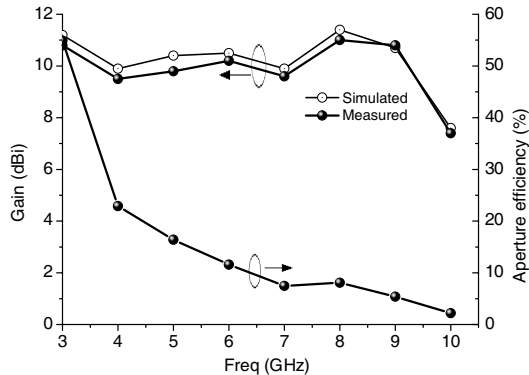


**Figure 6.** Gain variation and aperture efficiency against frequency for proposed antenna.

the  $E$ - and  $H$ -planes at 3, 5, 7 and 9 GHz are also compared and plotted in Figure 5. For the entire operating bands, it can be observed that the measured results have a maximum cross-polarization level of about  $-20$  dB of the  $E$  planes and about  $-15$  dB of the  $H$ -planes and the front-back ration is about 20 dB, and have good agreement with the simulations. Figure 6 shows the peak antenna gain for the proposed antenna. Over the whole band, the antenna gain is varied from about 7.4–10.8 dBi. The simulated aperture efficiency is also shown in Figure 6 which varies from 54% to 2% within the operating band. Due to non-uniform magnitude and phase reversal of some part of electric fields in the electrically large aperture, it deteriorates at higher frequencies.

#### 4. CONCLUSION

The ultra-wideband performance of a cavity-backed bowtie antenna with parasitic dipole and parasitic circular rings is presented and investigated. Using the parasitic dipole and parasitic circular ring to effectively improve the radiation patterns, the proposed antenna can achieve a stable broadside unidirectional radiation patterns. Ultra-wideband impedance characteristic of the antenna is obtained by the elliptical bowtie dipole and the taper feeding microstrip which can achieve an operating bandwidth of about 118.2% ranging from 2.75–10.7 GHz ( $VSWR \leq 2$ ). Due to these good performances, the antenna has wide and potential applications for indoor application of the recent wireless communication services.



## REFERENCES

1. Abbosh, A. M. and M. E. Bialkowski, "Design of ultra-wideband planar monopole antennas of circular and elliptical shape," *IEEE Trans. Antennas Propag.*, Vol. 56, 17–23, 2008.
2. Wu, Q., R. Jin, J. Geng, and M. Ding, "Printed omni-directional UWB monopole antenna with very compact size," *IEEE Trans. Antennas Propag.*, Vol. 56, 896–899, 2008.
3. Azarmanesh, M., S. Soltani, and P. Lotfi, "Design of an ultra-wideband monopole antenna with WiMAX, C and wireless local area network," *IET Microw. Antennas Propag.*, Vol. 5, 728–733, 2011.
4. Abbosh, A. M., H. K. Kan, and M. E. Bialkowski, "Compact ultra-wideband planar tapered slot antenna for use in a microwave imaging system," *Microw. Opt. Technol. Lett.*, Vol. 48, 2212–2216, 2006.
5. Reed, J., R. Michael Buehrer, and D. S. Ha, "Introduction to UWB: Impulse radio for radar and wireless communications," *MPRG*, 4, 2002.
6. Bialkowski, M. E. and A. M. Abbosh, "Design of UWB planar antenna with improved cut-off at the out-of-band frequencies," *IEEE Antennas Wirel. Propag. Lett.*, Vol. 7, 408–410, 2008.
7. Abbosh, A. M., "Miniaturized microstrip-fed tapered-slot antenna with ultrawideband performance," *IEEE Antennas Wirel. Propag. Lett.*, Vol. 8, 690–692, 2009.
8. Faraji, D. and M. N. Azarmanesh, "A novel modified head-shaped monopole antenna for UWB applications," *Journal of Electromagnetic Waves and Applications*, Vol. 23, No. 10, 1291–1301, 2009.
9. Ma, Q., B.-H. Sun, J.-F. Li, and Q.-Z. Liu, "A differential rectangular patch antenna with marchand balun for UWB applications," *Journal of Electromagnetic Waves and Applications*, Vol. 23, No. 1, 49–55, 2009.
10. Lee, S. H., J. N. Lee, J. K. Park, and H. S. Kim, "Design of the compact UWB antenna with PI-shaped matching stub," *Journal of Electromagnetic Waves and Applications*, Vol. 22, No. 10, 1440–1449, 2008.
11. Moosazadeh, M., C. Ghobadi, and M. Dousti, "Small monopole antenna with checkered-shaped patch for UWB application," *IEEE Antennas Wirel. Propag. Lett.*, Vol. 9, 1014–1017, 2010.
12. Siahcheshm, A., S. Sadat, C. Ghobadi, and J. Nourinia, "Design of a microstrip slot antenna filled by an isosceles triangle

- for UWB applications,” *Journal of Electromagnetic Waves and Applications*, Vol. 22, No. 1, 111–118, 2008.
13. Abbosh, A. M., “Miniaturization of planar ultrawideband antenna via corrugation,” *IEEE Antennas Wirel. Propag. Lett.*, Vol. 7, 685–688, 2008.
  14. Yang, C., Q. Guo, and K. Huang, “Study of a double-fed circular disc monopole antenna for UWB systems,” *Journal of Electromagnetic Waves and Applications*, Vol. 24, Nos. 14–15, 1943–1952, 2010.
  15. Lau, K. F. and K. M. Luk, “A wideband monopolar wire-patch antenna for indoor base station applications,” *IEEE Antennas Wirel. Propag. Lett.*, Vol. 4, 155–157, 2005.
  16. Row, J.-S., S.-H. Yeh, and K.-L. Wong, “A wide-band monopolar plate-patch antenna,” *IEEE Trans. Antennas Propag.*, Vol. 50, 1328–1330, 2002.
  17. Khan, S. N., J. Yao, Z. Shuai, and S. He, “Modified square UWB monopole antenna for improved impedance bandwidth,” *Journal of Electromagnetic Waves and Applications*, Vol. 22, Nos. 14–15, 1883–1888, 2008.
  18. Lau, K.-L. and K.-M. Luk, “Wideband folded L-slot shorted-patch antenna,” *Electron. Lett.*, Vol. 41, 1098–1099, 2005.
  19. Kumar, A. and H. D. Hristov, *Microwave Cavity Antennas*, Artech House, Norwood, MA, 1989.
  20. Li, R., D. Thompson, M. M. Tentzeris, J. Laskar, and J. Papapolymou, “Development of a wide-band short backfire antenna excited by an unbalance-fed H-shaped slot,” *IEEE Trans. Antennas Propag.*, Vol. 53, 662–671, 2005.
  21. Wong, J. L. and H. E. King, “A cavity-backed dipole antenna with wide bandwidth characteristics,” *IEEE Trans. Antennas Propag.*, Vol. 21, 725–727, 1973.
  22. Qu, S.-W., J.-L. Li, Q. Xue, C. H. Chan, and S. Li, “Wideband and unidirectional cavity-backed folded triangular bowtie antenna,” *IEEE Trans. Antennas Propag.*, Vol. 55, 1259–1263, 2009.
  23. Qu, S.-W., J.-L. Li, Q. Xue, and C. H. Chan, “Wideband cavity-backed bowtie antenna with pattern improvement,” *IEEE Trans. Antennas Propag.*, Vol. 56, 1259–1263, 2008.